Hindawi
Geofluids
Volume 2017, Article ID 5192473, 11 pages
https://doi.org/10.1155/2017/5192473

WILEY | Hindawi

Research Article

Modelling of River-Groundwater Interactions under Rainfall Events Based on a Modified Tank Model

Wen Nie,[1,2] Yong-chang Liang,[3] Lin Chen,[4] and Wei Shao[5]

[1]*State Key Laboratory of Geo-Hazard Prevention and Geo-Environment Protection, Chengdu University of Technology, Chengdu 610059, China*
[2]*Quanzhou Institute of Equipment Manufacturing, Haixi Institutes, Chinese Academy of Sciences, Quanzhou 362200, China*
[3]*State Key Laboratory of Oil and Gas Reservoir Geology and Exploitation, Southwest Petroleum University, Chengdu, Sichuan 610500, China*
[4]*College of Science, Southwest Petroleum University, Chengdu, Sichuan 610500, China*
[5]*College of Hydrometeorology, Nanjing University of Information Science and Technology, Nanjing, Jiangsu 210044, China*

Correspondence should be addressed to Wen Nie; niewen1026@gmail.com

Received 12 January 2017; Revised 8 May 2017; Accepted 28 May 2017; Published 2 July 2017

Academic Editor: Kundan Kumar

A multitank model experiment is employed to simulate the river-groundwater interaction under rainfall events. These experiments involve coarse and fine materials and rainfall events of 45 and 65 mm/hr. We developed a modified tank model for estimation of the groundwater table and river levels in these experiments. Parameter training of our tank model includes two algorithms: (i) the nonincremental learning algorithm-based model can predict the pore water pressure (PWP) in a slope and river under a 65 mm/hr rainfall event (coarse material) with Nash–Sutcliffe efficiency (NSE) = 0.427 and −0.909 and (ii) the incremental learning algorithm-based model can predict the PWP in a slope and river with NSE = 0.994 and 0.995. Then, the river-groundwater interaction was reproduced by a numerical case. The results of the deterministic method of the numerical case and optimized method of the modified tank model matched well.

1. Introduction

River-groundwater interaction of river-slope systems under rainfall events is common in riverbank and basin areas. The general process is described in Figure 1. Estimation of groundwater is usually complicated as a result of groundwater-river interactions, which could relate to the permeability, hydraulic gradients, and hydrogeological properties in the slope-river system [1–5]. The hydrological processes of the river-slope system are strongly linked to stream flow generation, contamination transport, and slope stability [2–10]. The deterministic method commonly uses the Darcy-Richards equation or the Boussinesq equation as hydrological models to simulate the groundwater flow in a slope [9], and the models can be further extended to dual-permeability models for preferential flow simulations [10, 11]. These hydrological models may be integrated with solute transport models to analyse contamination risks [12] or with soil mechanics models for slope stability analysis [10, 11]. However, solving the deterministic models numerically is usually computationally expensive, and the implementation requires detailed investigation of the geometries and hydraulic properties of the slope material [11]. Compared to the deterministic method, a model based on an optimized method such as the tank model [6] usually does not need material information about permeability and infiltration. It uses historical monitoring data for estimating or training parameters of the assumed model structure [7, 8]. In other words, the method only needs the historical data to carry out parameter estimation for the relation between the input and output of the model. Then the parameters estimated can help decide objectives like groundwater by inputting infiltration. Therefore, these optimized methods can be applied to a wide range of different landslide settings, and we estimate that, for more than 90% of

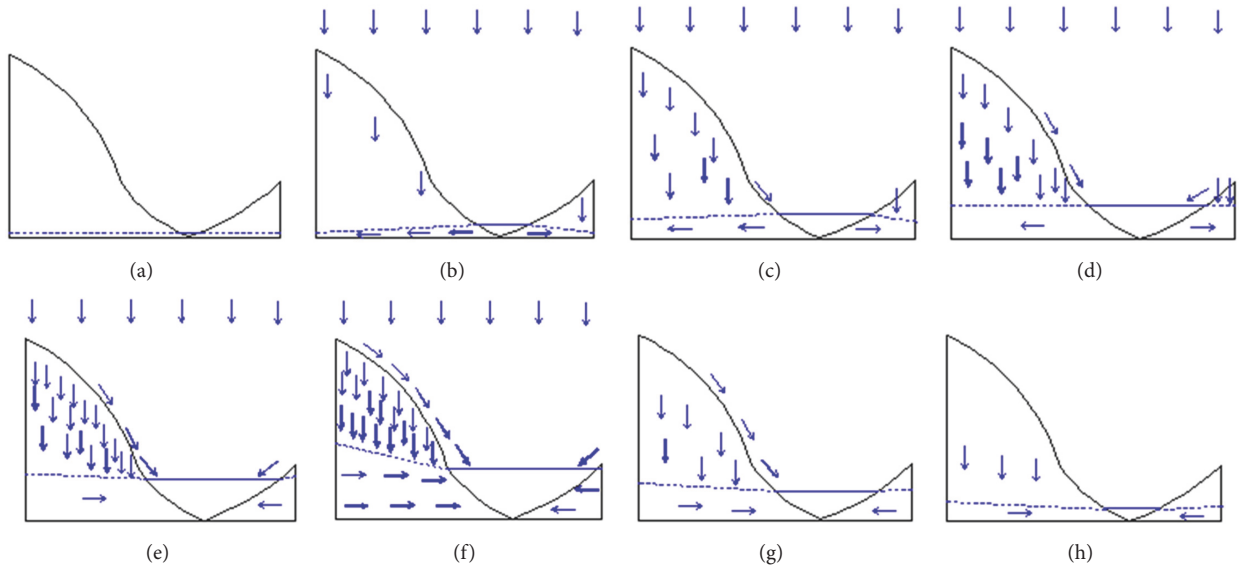

Figure 1: River-groundwater interaction under rainfall event: (a) initial state; (b) groundwater level raised by rainfall infiltration and river supply; (c) more rainfall and river supply and overland flow produced; (d) high groundwater table produced by continuous rainfall; (e) groundwater conversely supplies the river level; (f) increased groundwater accelerates the water flow supply to river; (g) overland flow and rainfall infiltration decrease; (h) recovery to the initial state.

all landslides, no explicit parameters for soil suction and so on are available. In our study, a series of physical multitank model experiments are carried out by simulating groundwater table changes in consideration of groundwater-river interactions under rainfall events. A modified conceptual tank model is used to predict the groundwater changes in these experiments. Parameter training in a modified tank model is involved with two algorithms (nonincremental and incremental learning algorithm). Then a numerical case based on the deterministic method is compared to our modified tank model. The remainder of the paper is organized as follows: Section 2 describes the original tank model and our modified tank model. Section 3 introduces the materials, device, and experimental procedure. Section 4 highlights the results of models of experiments and analysis of the original and modified conceptual tank model. The performance of the modified tank model with the nonincremental and incremental learning algorithms is introduced and discussed in Section 5. Section 6 discusses the replicated application of the modified tank models by a numerical riverbank simulation. The conclusions are detailed in Section 7.

2. Original and Modified Tank Models

A tank model is a nonlinear theorized calculation to describe the behaviours of water hydraulic properties [6]. Until now, simple or multitank models have been used for estimation of groundwater in a homogenous slope involving many experimental or real cases [13–18]. The basic mechanism of the multitank model is as shown in Figure 2(a).

Equation (1) indicates the change of groundwater table related to infiltration and drainage in a unit of time in every tank element. Equation (2) shows the infiltration affected by the perched water table. Equation (3) shows the drainage rate affected by the current groundwater table.

$$\begin{aligned} W_1(t+1) - W_1(t) &= I_1(t), \\ W_2(t+1) - W_2(t) &= I_2(t) - Q_2(t), \\ W_3(t+1) - W_3(t) &= I_3(t), \\ W_4(t+1) - W_4(t) &= I_4(t) - Q_4(t) + Q_2(t), \end{aligned} \tag{1}$$

$$\begin{aligned} I_2(t) &= b_1 W_1(t), \\ I_4(t) &= b_2 W_3(t), \end{aligned} \tag{2}$$

$$\begin{aligned} Q_2(t) &= a_2 W_2(t), \\ Q_4(t) &= a_4 W_4(t), \end{aligned} \tag{3}$$

where t and $t + 1$ are the time steps, I_j is the infiltration, W_j is the water table, Q_j is defined as drainage, a_j is a coefficient indicating the relation between drainage and the groundwater table, j is 1, 2, 3, and 4, and b_1 and b_2 are the coefficients indicating the relation between surface infiltration and a perched water table.

Compared to the original tank model, our modified tank model simplifies the structure of the tank model (Figure 2(b)). It considers the maximum infiltration ability and time lag of groundwater induced by the path, material, and moisture content in the previous condition.

$$\begin{aligned} W_1(t+1) - W_1(t) &= a_1 I_1(t+\Delta) - Q_{1\text{-}2}(t), \\ W_2(t+1) - W_2(t) &= a_2 I_2(t+\Delta) + Q_{1\text{-}2}(t+\Delta_1) \\ &\quad - Q_2(t), \end{aligned} \tag{4}$$

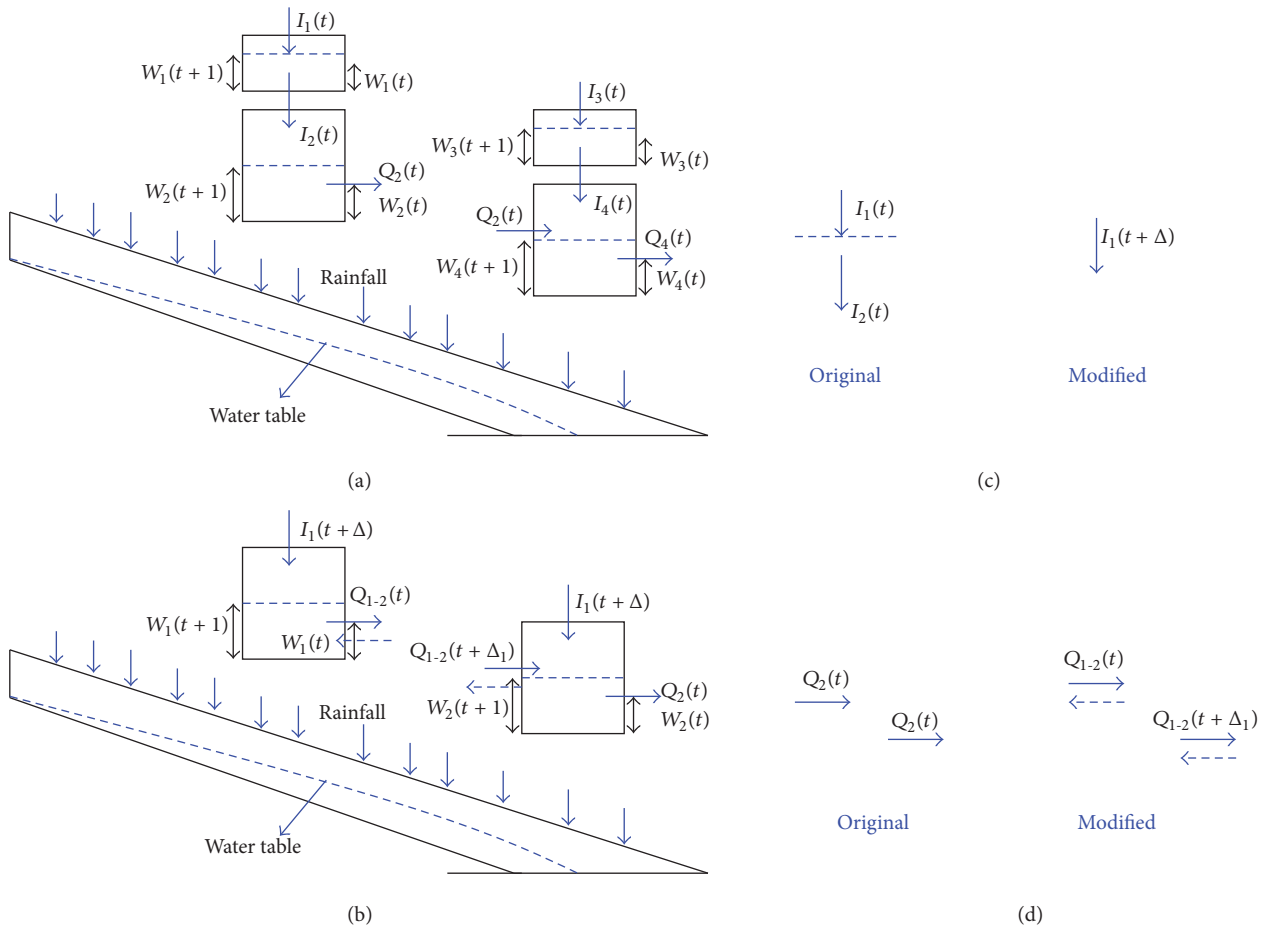

FIGURE 2: Comparison of original and modified multistorage tank models: (a) original multistorage tank model; (b) modified multistorage tank model; (c) optimizing the infiltration time lag; (d) optimizing the lateral water flow time lag.

$$
\begin{aligned}
Q_{1\text{-}2}(t) &= b_{1\text{-}2}\left(W_1(t) - W_2(t)\right), \\
Q_{1\text{-}2}\left(t+\Delta_1\right) &= b_{2\text{-}1}\left(W_1(t) - W_2(t)\right), \\
Q_2(t) &= b_2 W_2(t).
\end{aligned} \tag{5}
$$

Equation (4) indicates the change of the groundwater table in a unit of time in every tank element. These equations consider the time lags resulting from the permeability, infiltration path, and water flow path. Equation (5) shows that the middle water flow supply ($Q_{1\text{-}2}(t)$ and $Q_{1\text{-}2}(t+\Delta_1)$) depends on the deviation of the water head pressure of two object points, which means that the water flow supply has no fixed direction and in the meantime still has a time lag (the dotted arrow represents a reversible process). The drainage rate ($Q_2(t)$) is affected by the current groundwater table. Specifically, in Figure 2(c), the original tank model calculates the infiltration time lag by increasing the number of tanks in a vertical direction, which introduces more parameters in the model. Meanwhile, the modified tank model innovatively calculates the infiltration time lag before rainfall enters the tank. "Δ" is the time lag between the infiltration and the water table induced by it. The time lag can be obtained by analysing the correlation between the water table and infiltration in unit time [19, 20]. In Figure 2(d), the original does not consider the short time lag of lateral water flow. The modified tank model considers the lateral water flow time lag of "Δ_1." This time lag can be overcome by the different parameter estimations of $b_{1\text{-}2}$ and $b_{2\text{-}1}$. Furthermore, in the modified tank model, the direction of lateral water flow depends on the balance of both water tables in the tanks.

3. Experiments and Predictive Model

River-slope system modelling includes a surface tank (surface runoff) and double tanks (slope and river), as shown in Figure 3. Rainfall is simulated by nozzles. Two pore water pressure (PWP) sensors are installed at the bottom of the double tanks for pore water pressure monitoring (model number CYY2, Xi'an Weizheng Technology Corp., Xi'an, China) (diameter: 3 cm; height: 1.6 cm; measuring range: ±10 kPa; deviation: ±0.2%). The drainage of this system is realized by a drain hole. Two types of material from Fengdu Ming Mountain, near Yangtze River Bank, Chongqing, China, are used (shown in Figures 4(a) and 4(b)). The particle-size distribution curves are shown in Figure 4(c). For each group of tank model experiments, we arranged two rainfall events (45 and 65 mm/hr intensity, 36 min duration) and the observation time was 1 hr. Every test in each group was

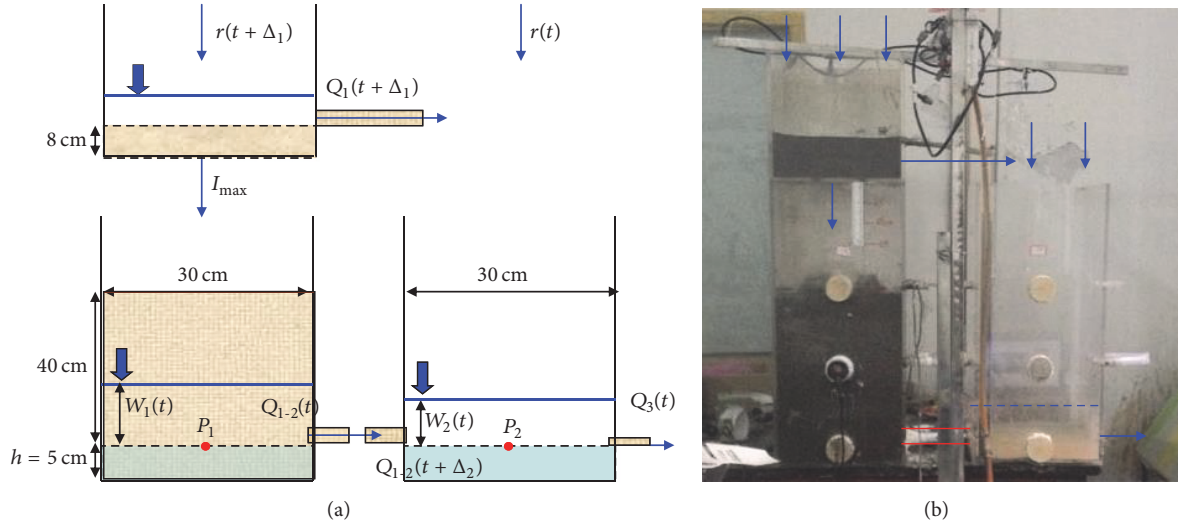

Figure 3: River-slope system modelling: (a) schematic diagram and (b) real scene.

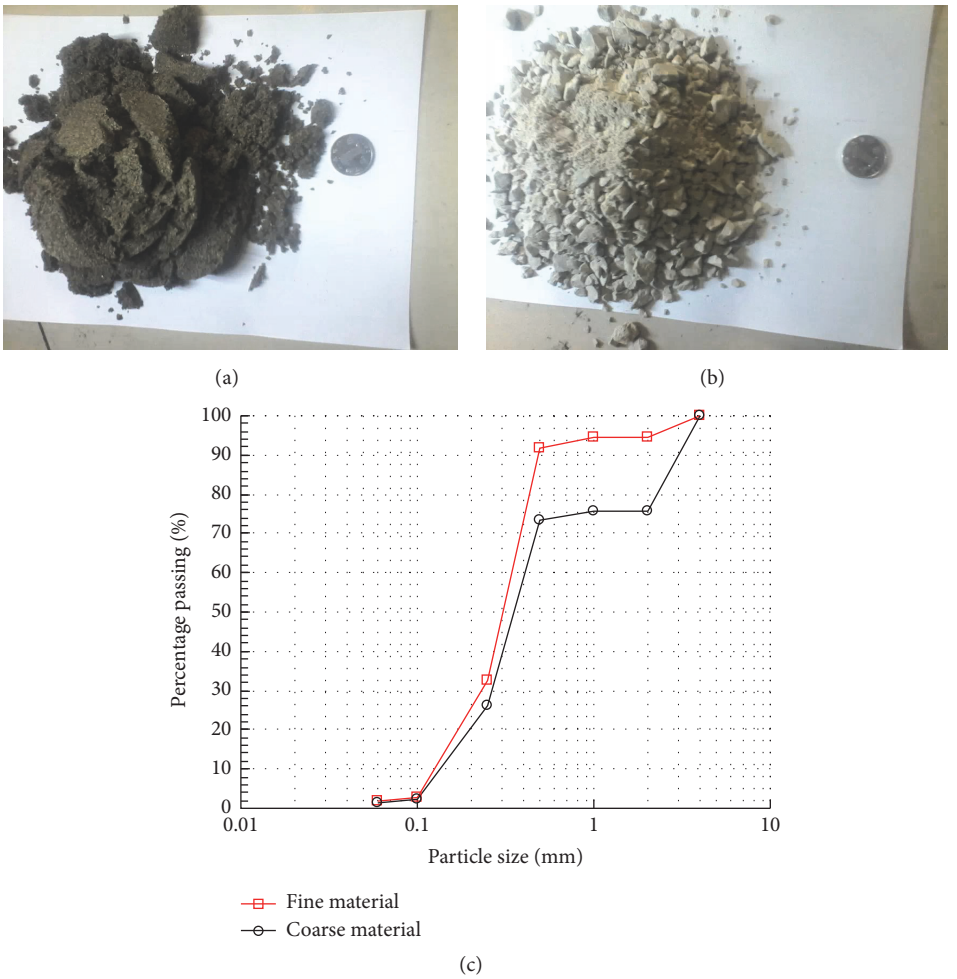

Figure 4: Schematic diagram of modified tank model system: (a) fine material; (b) coarse material; (c) particle-size distribution curves.

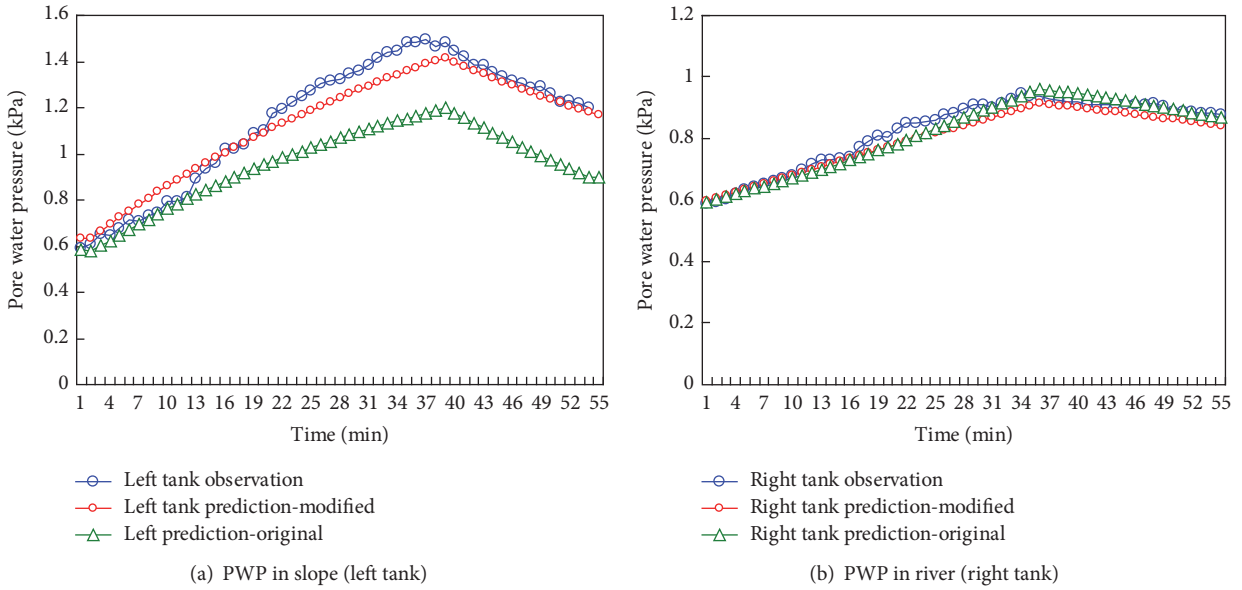

(a) PWP in slope (left tank)

(b) PWP in river (right tank)

Figure 5: Predictions of original and modified tank models (fine material): (a) PWP in slope and (b) PWP in river.

conducted under similar initial conditions, such as geometry, material, and initial moisture content, which was tested by a moisture transducer in the bottom (model number DS200, Beijing Dingtek Technology Corp., Beijing, China) (frequency domain sensors: measuring range: 0–100%; resolution: 0.1%; deviation: ±2%; with a soil contact area of less than 20 mm^2; deviation: ±3%).

Equation (6) indicates the ground water table and river level in the river-slope system in Figure 5.

$$W_1(t+1) - W_1(t) = \left(r\left(t+\Delta_1\right) - Q_1\left(t+\Delta_1\right)\right) - Q_{1\text{-}2}(t), \quad (6)$$

$$W_2(t+1) - W_2(t) = r(t) + Q_{1\text{-}2}\left(t+\Delta_2\right) - Q_3(t),$$

where $W_1(t+1)$ and $W_1(t)$ are the water table in the slope at times $t+1$ and t; $W_2(t+1)$ and $W_2(t)$ are the water level of the river at times $t+1$ and t; $r(t+\Delta_1)$ and $Q_1(t+\Delta_1)$ are the rainfall and surface runoff at time $t+\Delta_1$; Δ_1 is the infiltration time lag produced by the path, material permeability, and previous moisture content. $Q_{1\text{-}2}(t)$ is the water flow between the slope and river at time t; $Q_{1\text{-}2}(t+\Delta_2)$ is the water flow between slope and river at time $t+\Delta_2$; $Q_3(t)$ is the drainage at time t.

The surface runoff, drainage, and water flow exchanges, which mainly depend on the pressure water head, are expressed by

$$Q_3(t) = b_2 P_2(t),$$

$$Q_{1\text{-}2}(t) = a_{1\text{-}2}\left(P_1(t) - P_2(t)\right), \quad (7)$$

$$Q_{1\text{-}2}\left(t+\Delta_2\right) = a_{2\text{-}1}\left(P_1(t) - P_2(t)\right).$$

The water table cannot usually be measured directly by sensors and is often proportional to pore water pressure. Thus, the final equation (8) is used to calculate the PWP changes in both slope and river.

$$P_1(t+1) - P_1(t) = a_1\left(r\left(t+\Delta_1\right) - Q_1\left(t+\Delta_1\right)\right) - a_{1\text{-}2}\left(P_1(t) - P_2(t)\right),$$

$$P_2(t+1) - P_2(t) = a_2\left(r(t) + Q_1\left(t+\Delta_1\right)\right) + a_{2\text{-}1}\left(P_1(t) - P_2(t)\right) - b_2 P_2(t), \quad (8)$$

where $P_1(t+1)$ and $P_1(t)$ are the PWP in the slope at times $t+1$ and t; $P_2(t+1)$ and $P_2(t)$ are the PWP of the river bottom at times $t+1$ and t; a_1, a_2, $a_{1\text{-}2}$, $a_{2\text{-}1}$, and b_2 are the relation coefficients. In the high water content layer, the time lag of water flow is relatively low; thus, we use the different coefficients $a_{1\text{-}2}$ and $a_{2\text{-}1}$ to refine it.

It should be pointed out that the major part of PWP could be static pressure induced by the water table height. Minor components are seepage force and the difference in pressures in the available pore space during drier and wetter periods. Since the tank model is a "grey box model," we do not know the exact proportions of static pressure, seepage pressure, and pressure dynamics in pore space, but all three are included in our equivalent pore water pressure.

4. A Comparison of the Original and Modified Tank Models

In this section, the performance of the original and modified tank models in physical experiments is shown and we

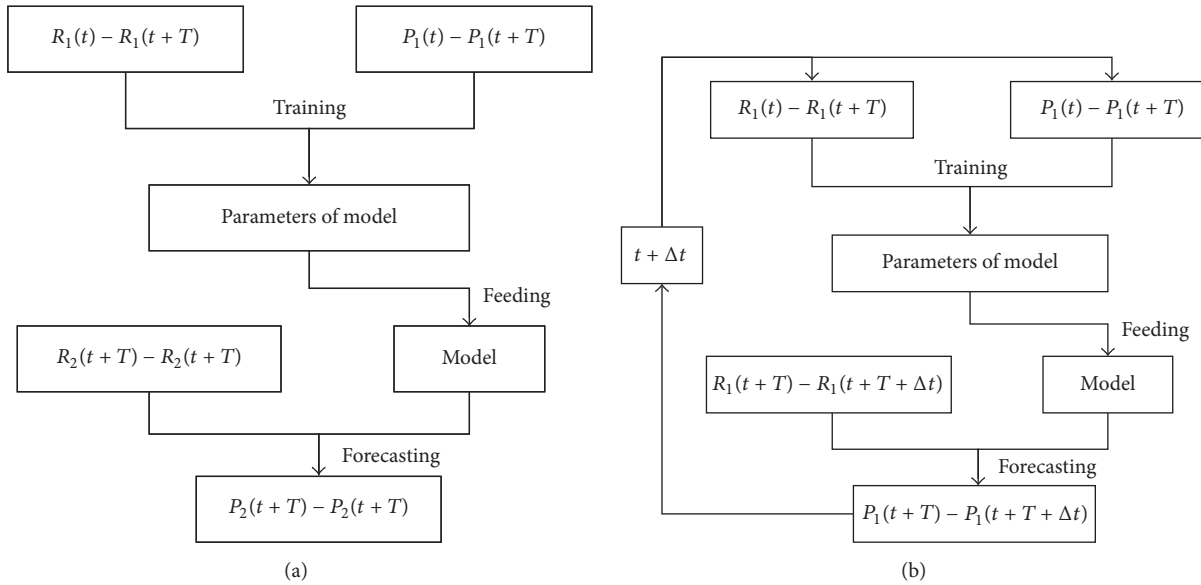

Figure 6: Comparison of calculations of parameters as constants and as variables: (a) nonincremental learning algorithm for parameters as constants and (b) incremental learning algorithm for parameters as variables.

introduce the standard Nash–Sutcliffe efficiency (NSE) [21], which is the most widely used criterion for calibration and evaluation of hydrological models with observed data. NSE is dimensionless and is scaled onto the interval [negative infinity to 1.0]. NSE is taken to be the "mean of the observations" [22] and if NSE is smaller than 0, the model is no better than using the observed mean as a predictor. Monitoring data (rainfall and PWP) from physical experiments of an event with a rainfall intensity of 45 mm/hr are employed to estimate the parameters of the original and modified models. The monitoring data (PWP) from the event with a rainfall intensity of 65 mm/hr are used to validate the predictions of the original and modified models. Figure 6 shows the results of the original and modified tank models (fine material).

In Figure 5(a), the left tank means the slope part of the river-slope system. The original tank model does not consider the groundwater-river exchanges. It only considers the water flows from the slope to the river. Thus, in the left tank, the water table is underestimated. In contrast, the modified tank model considers the supply from the river in the beginning. Therefore, the reduction of the PWP is slow, which matches the real situation well. The NSE of the original tank model is 0.438, while the NSE of the modified tank model is 0.973. In Figure 5(b), the right tank represents the river part of the river-slope system. It is found that both the original and modified tank models can describe the process well. This may be because the water level is not so sensitive to amount of rainfall added to the river compared to porosity material-soil mass. In other words, adding the same amount of rainfall can lead to a groundwater table in the soil that is higher than the river level, which also produces more prediction errors because of the porosity. Thus, the error of river level estimation is not obvious for either model. The NSE of the original tank model is 0.972 while that of the modified tank model is 0.955.

5. Nonincremental Constants and Incremental Learning Algorithm Variables in the Modified Tank Model

In this section, the performance of nonincremental constants and incremental learning algorithm variables in a modified tank model are shown and the NSE is still used to evaluate the use of two types of parameters that affect the modified tank model. An incremental learning algorithm is introduced which considers the parameters of the modified tank model as variables instead of constants [23]. The same terminology is used in computer science for machine learning, where model parameters are tuned using an abundance of observations. In other words, we used the previous observed values to train the parameters of the model to predict the object in the next time domain and then repeated the process in the following time domain, which is similar to the dynamically updated method. A comparison of calculations of parameters as constants and as variables is shown in Figure 6. We use the coarse material experiments to show the process.

For the nonincremental learning algorithm, R_1 and P_1 are all the monitoring data from rainfall event 1, which consist of rainfall and PWP under different time domains ($t \cdots T$). All the data are used to train the parameters of the model (constant parameters). Then these parameters are fed into the model. When the new rainfall event R_2 is input into the model, it can make predictions of P_2 under different time domains. For the incremental learning algorithm, parts of R_1 and P_1, such as data under t to $t + T$, are used to train the parameters of the model. After tuning the parameters, the model can predict the next P_1 under $t + T + \Delta t$ in the same rainfall event by reading the rainfall R_1 under the time domain $t + T + \Delta t$. Then, the new monitoring data under time domain $t + \Delta t + T + \Delta t$ are used to train the parameters again

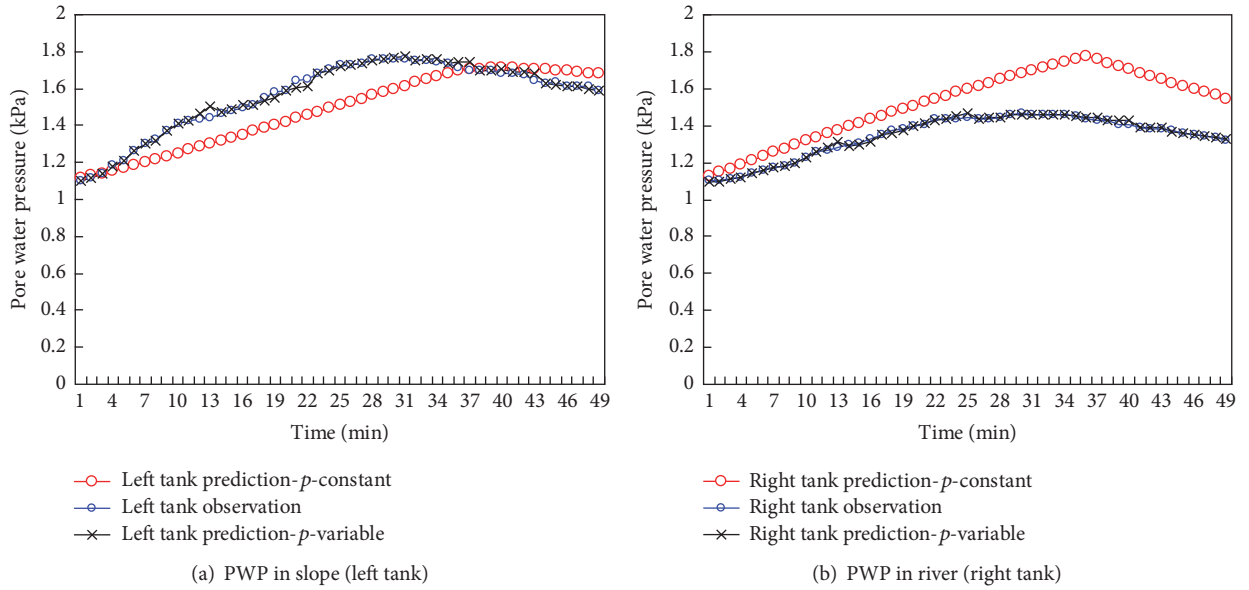

(a) PWP in slope (left tank) (b) PWP in river (right tank)

Figure 7: A comparison of nonincremental and incremental learning algorithms: (a) PWP in slope and (b) PWP in river.

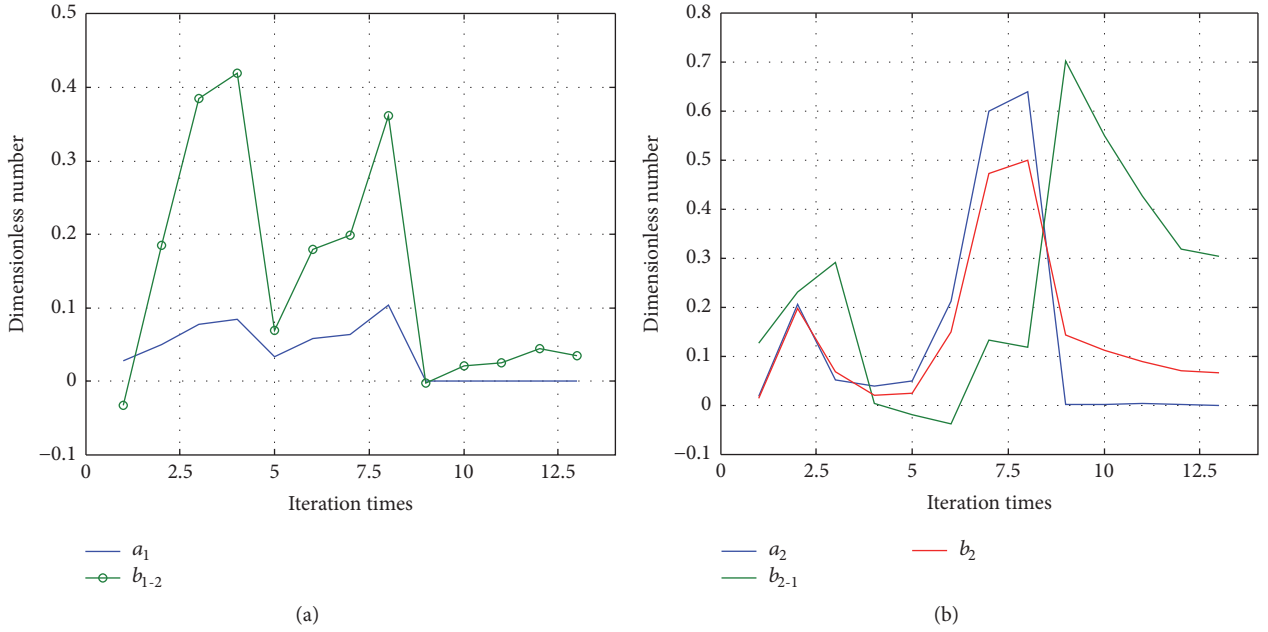

(a) (b)

Figure 8: Changes of parameters in incremental learning algorithm: (a) parameters in the left tank and (b) parameters in the right tank.

(variable parameters) and then make the new prediction. The cyclic action means that incremental learning takes place.

Figure 7 shows the performances of the models based on the parameter types resulting from the two learning algorithms (nonincremental constants and incremental learning algorithm).

The distribution of pores in coarse material is more uncertain than that in fine materials. Thus, the error of the modified tank model using constant parameters is obvious. The NSEs of the modified tank model with constant parameters are 0.427 and −0.909. As shown in Figure 7, using the incremental learning algorithm, the modified tank model with variable parameters has higher NSEs of 0.994 and 0.995 in the slope and river, respectively. The model based on the incremental learning algorithm can more accurately predict the PWP trend but requires continuous parameter estimation. By contrast, the model based on the nonincremental learning algorithm only needs to carry out parameter estimation once based on historical data but sometimes has low accuracy.

Figure 8 indicates the changes of parameters when using the incremental learning algorithm.

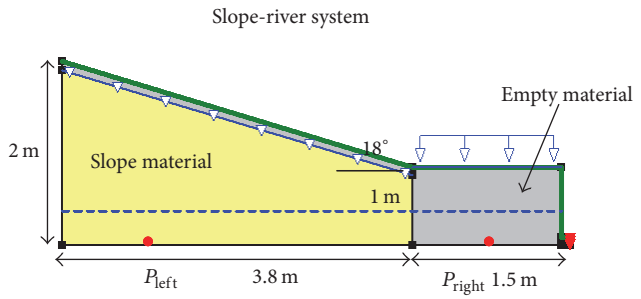

Figure 9: Geometry of numerical model.

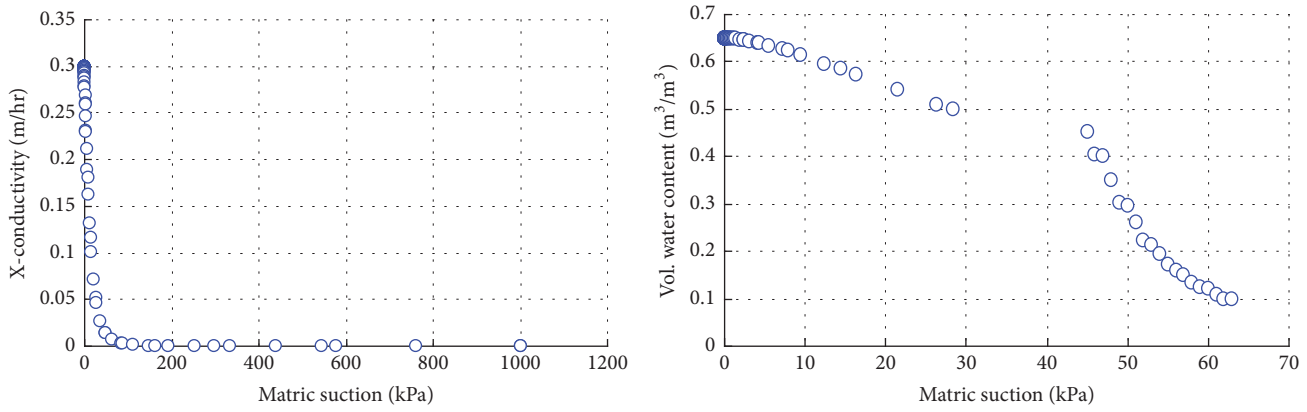

Figure 10: Permeability coefficient (fine material): (a) matric suction versus conductivity and (b) matric suction versus water content.

It is found that the parameters basically reflect the change of the PWP trend.

(1) a_1 (PWP sensitivity to rainfall): an increase means the PWP accelerates upward; a decrease means the PWP rate decreases.

(2) $b_{1\text{-}2}$: an increase means a high water flow output, while a decrease means a low water flow output.

(3) a_2 (PWP sensitivity to rainfall): an increase means that the PWP accelerates upward; a decrease means that the PWP rate decreases.

(4) $b_{2\text{-}1}$: an increase means a high water flow input while a decrease means a low water flow input. b_2: an increase means a high drainage rate while a decrease means a low drainage rate.

6. Replication of Numerical Model

Numerical slopes using the transient groundwater mode of SEEP/W [24] are employed to reproduce the applications of our modified tank model. The estimation of matric suction and conductivity uses Fredlund and Xing's method [25], as shown in Figures 10(a) and 13(a). The link between matric suction and water content uses the model in Kunze et al. [26], as shown in Figures 10(b) and 13(b). In Figure 9, the slope is 2 m deep and 3.8 m long with an angle of 18 degrees and homogeneous materials (main mass). The empty material and the surface layer have high permeability ($1 - e4$ m/s). The residual (99%) and initial water content (99.99%) in them are very close when simulating the river basin and surface runoff path. The design ensures that the rainfall and potential surface runoff flow into the river swiftly. The toe of the river basin has a drainage point (the pressure head is 0 m). The grid size is 0.1 m × 0.1 m. The observation time of the process is 4 hours and the rainfall input lasts 1 hr. The procedures involving fine and coarse materials are as follows:

(1) P_{left} (pore water pressure in the slope) and P_{right} (pore water pressure in the river) under rainfall of 45 mm/hr are used as training data for the parameters of the modified tank model.

(2) P_{left} and P_{right} induced by a rainfall event of 65 mm/hr are predicted using the modified tank model.

The slope part and the river part are treated as a double tank (the left tank is the slope part; the right tank is the river part). Figure 11 indicates the change of the PWP in the left and right tanks under rainfall intensities of 45 and 65 mm/hr. Figure 12 indicates prediction of the modified tank model based on the parameters from the nonincremental learning algorithm.

Figure 14 indicates the change of PWP in the left and right tanks under rainfall intensities of 45 and 65 mm/hr. Figure 15 indicates the prediction of the modified tank model based on the parameters given by the nonincremental learning algorithm.

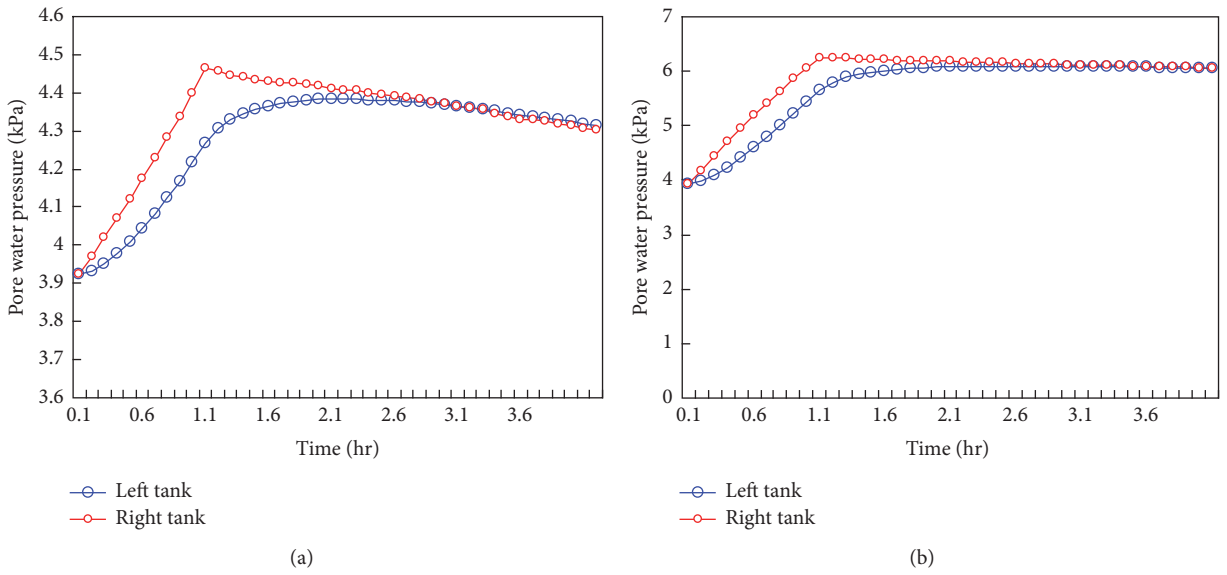

Figure 11: Monitoring data of numerical model (fine materials): (a) 45 mm/hr rainfall intensity and (b) 65 mm/hr rainfall intensity.

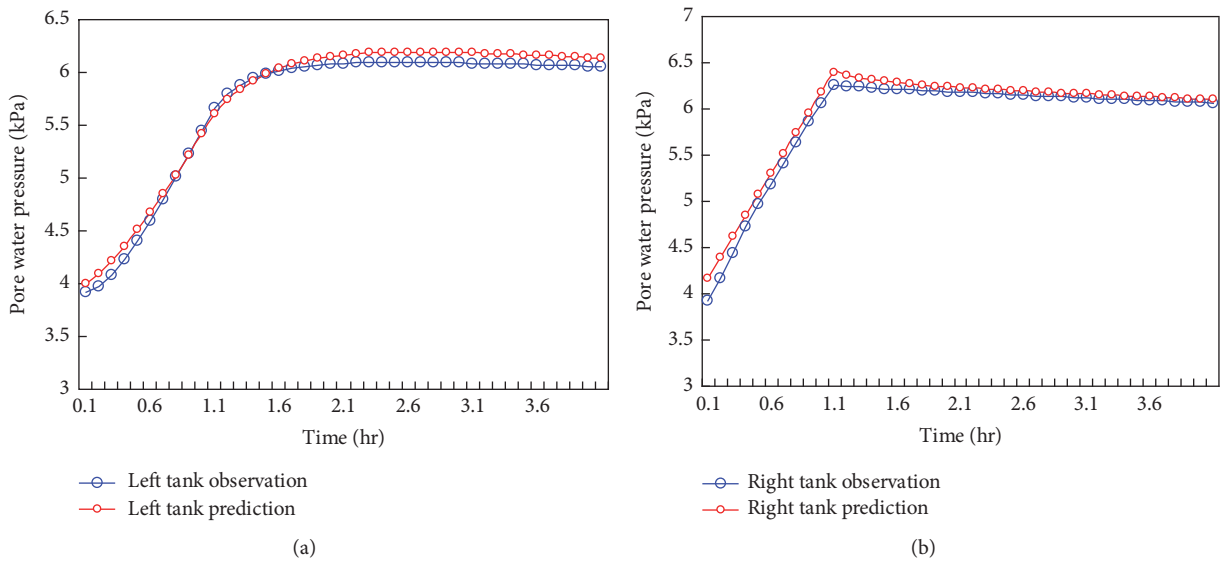

Figure 12: Prediction by modified tank model (fine material): (a) left tank and (b) right tank.

7. Concluding Remarks

Modelling of river-groundwater interactions under rainfall events is executed based on tank model experiments. These experiments involve fine (coarse) materials and rainfall intensities of 45 and 65 mm/hr. We developed modified tank models with nonincremental and incremental learning algorithms to describe the process. A numerical case reproduces the river-groundwater interactions and validates the prediction by our modified model. Future work will take the direction of obtaining field measurements in order to compare model predictions against field observations.

Currently, the valuable conclusions include the following:

(1) The modified tank model not only describes the changes of PWP in the slope and river more accurately than the original model but also has a simpler structure.

(2) The model based on the incremental learning algorithm can more accurately predict the PWP trend but needs continuous parameter estimation. The model based on the nonincremental learning algorithm only needs to perform parameter estimation once, based on historical data, but has low accuracy.

(3) The modified tank model can match the deterministic method well based on the numerical model case.

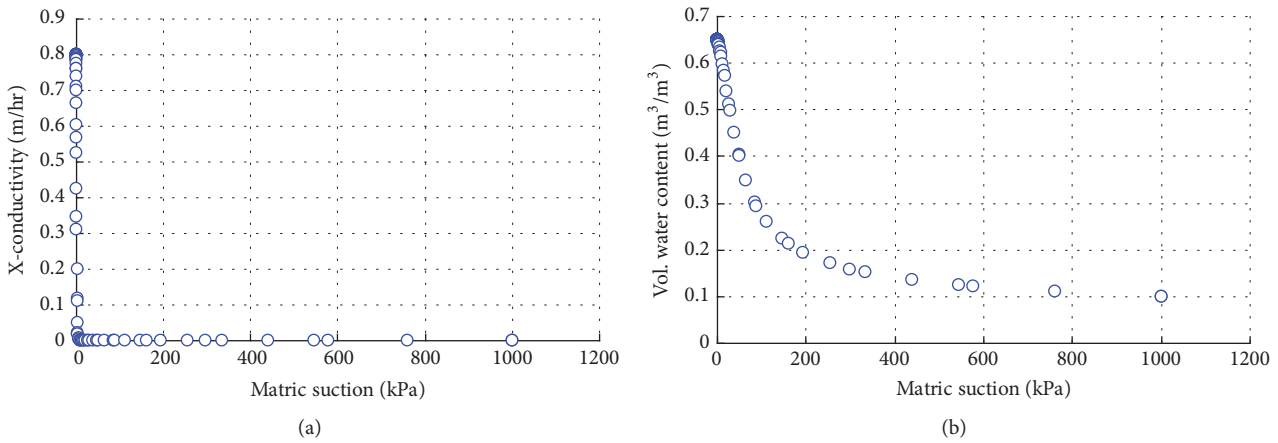

Figure 13: Permeability coefficient (coarse material): (a) matric suction versus conductivity and (b) matric suction versus water content.

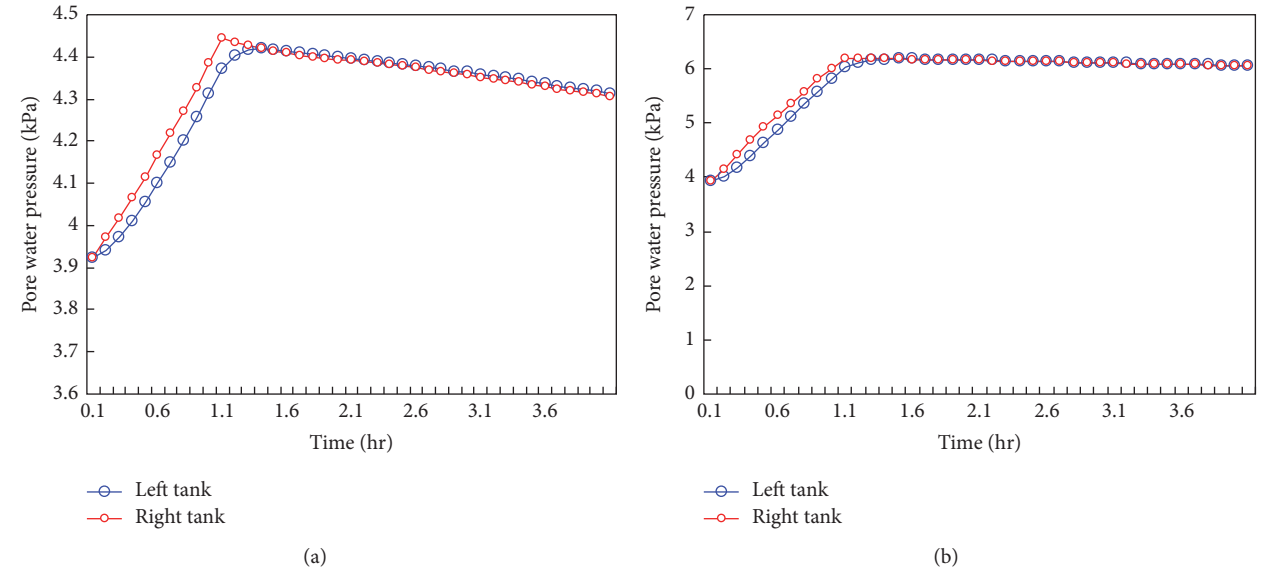

Figure 14: Monitoring data of numerical model (coarse materials): (a) 45 mm/hr rainfall intensity and (b) 65 mm/hr rainfall intensity.

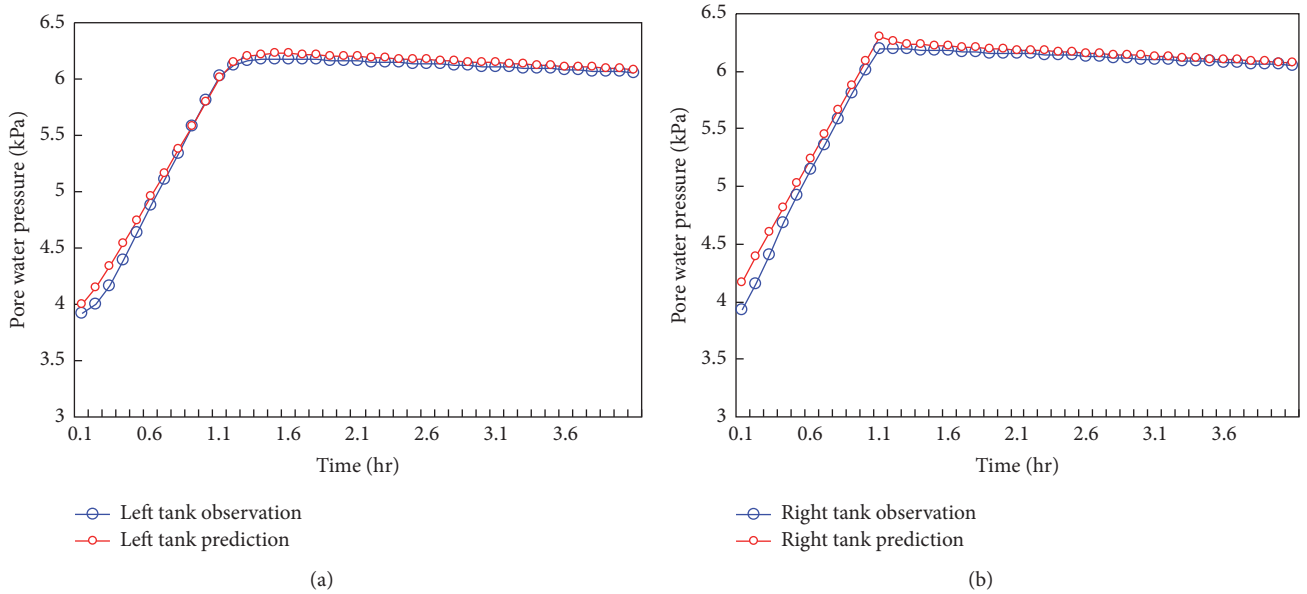

Figure 15: Prediction by modified tank model (coarse material): (a) left tank and (b) right tank.

Conflicts of Interest

The authors declare that they have no conflicts of interest.

Acknowledgments

The research is supported by the Opening Fund of the State Key Laboratory of Geo-Hazard Prevention and Geo-Environment Protection (Chengdu University of Technology), SKLGP2017K006.

References

[1] M. Trémolières, I. Eglin, U. Roeck, and R. Carbiener, "The exchange process between river and groundwater on the Central Alsace floodplain (Eastern France)—I. The case of the canalised river Rhine," *Hydrobiologia*, vol. 254, no. 3, pp. 133–148, 1993.

[2] C. Doussan, E. Ledoux, and M. Detay, "River-groundwater exchanges, bank filtration, and groundwater quality: Ammonium behavior," *Journal of Environmental Quality*, vol. 27, no. 6, pp. 1418–1427, 1998.

[3] W. D. Gollnitz, "Infiltration rate variability and research needs," in *Riverbank Filtration*, pp. 281–290, Springer, Amsterdam, The Netherlands, 2003.

[4] D. O. Rosenberry and R. W. Healy, "Influence of a thin veneer of low-hydraulic-conductivity sediment on modelled exchange between river water and groundwater in response to induced infiltration," *Hydrological Processes*, vol. 26, no. 4, pp. 544–557, 2012.

[5] S. Mutiti and J. Levy, "Using temperature modeling to investigate the temporal variability of riverbed hydraulic conductivity during storm events," *Journal of Hydrology*, vol. 388, no. 3-4, pp. 321–334, 2010.

[6] Y. Ishihara and S. Kobatake, "Runoff Model for Flood Forecasting," *Bulletin of the Disaster Prevention Research Institute*, vol. 29, no. 1, pp. 27–43, 1979.

[7] F. Faris and F. Fathani, "A coupled hydrology/slope kinematics model for developing early warning criteria in the Kalitlaga Landslide, Banjarnegara, Indonesia," in *Progress of Geo-Disaster Mitigation Technology in Asia*, pp. 453–467, Springer, Berlin, Germany, 2013.

[8] N. A. Abebe, F. L. Ogden, and N. R. Pradhan, "Sensitivity and uncertainty analysis of the conceptual HBV rainfall-runoff model: Implications for parameter estimation," *Journal of Hydrology*, vol. 389, no. 3-4, pp. 301–310, 2010.

[9] S. K. Kampf and S. J. Burges, "A framework for classifying and comparing distributed hillslope and catchment hydrologic models," *Water Resources Research*, vol. 43, no. 5, Article ID W05423, 2007.

[10] W. Shao, T. A. Bogaard, M. Bakker, and R. Greco, "Quantification of the influence of preferential flow on slope stability using a numerical modelling approach," *Hydrology and Earth System Sciences*, vol. 19, no. 5, pp. 2197–2212, 2015.

[11] W. Shao, T. Bogaard, M. Bakker, and M. Berti, "The influence of preferential flow on pressure propagation and landslide triggering of the Rocca Pitigliana landslide," *Journal of Hydrology*, vol. 543, pp. 360–372, 2016.

[12] J. M. Köhne, S. Köhne, and J. Šimůnek, "A review of model applications for structured soils: a water flow and tracer transport," *Journal of Contaminant Hydrology*, vol. 104, no. 1–4, pp. 4–35, 2009.

[13] M. Nishihgaki, *Research on behavior of groundwater and its application to foundation engineering [M.S. thesis]*, Kyoto University, Kyoto, Japan, 1979.

[14] M. Michiue, "A method for predicting slope failures on cliff and mountain due to heavy rain," *Natural Disaster Science*, vol. 7, no. 1, pp. 1–12, 1985.

[15] K. Takahashi, Y. Ohnish, J. Xiong, and T. Koyama, "Tank model and its application to groundwater table prediction of slope," *Chinese Journal of Rock Mechanics and Engineering*, vol. 27, no. 12, pp. 2501–2508, 2008.

[16] K. Takahashi, *Research of underground water numerical analysis method that considering water circulation system [Ph.D. thesis]*, Department of Urban and Environmental Engineering, Kyoto University, Kyoto, Japan, 2004.

[17] J. Xiong, Y. Ohnish, K. Takahashi, and T. Koyama, "Parameter determination of multi-tank model with dynamically dimensioned search," in *Proceedings of the Symposium Rock Mechanics*, vol. 38, pp. 19–24, Japan, 2009.

[18] T. Ichimura, T. Ryohei, and S. Daiken, "Evaluation of hydraulic properties of slope ground based on monitoring data of moisture contents," in *Proseedings of the 4th Japan–Taiwan Joint Workshop on Geotechnical Hazards from Large Earthquakes and Heavy Rainfalls*, Sendai, Japan.

[19] S. Matsuura, S. Asano, and T. Okamoto, "Relationship between rain and/or meltwater, pore-water pressure and displacement of a reactivated landslide," *Engineering Geology*, vol. 101, no. 1-2, pp. 49–59, 2008.

[20] W. Nie, M. Krautblatter, and K. Thuro, "Porenwasserdruckänderungen aufgrund von Regen und Schneeschmelze in einer tiefgreifenden Massenbewegung," 2013.

[21] J. E. Nash and J. V. Sutcliffe, "River flow forecasting through conceptual models part I—a discussion of principles," *Journal of Hydrology*, vol. 10, no. 3, pp. 282–290, 1970.

[22] A. H. Murphy, "Skill scores based on the mean square error and their relationships to the correlation coefficient," *Monthly Weather Review*, vol. 116, no. 12, pp. 2417–2424, 1988.

[23] W. Nie, R. Q. Huang, Q. G. Zhang, W. Xian, F. L. Xu, and L. Chen, "Prediction of experimental rainfall-eroded soil area based on S-shaped growth curve model framework," *Applied Sciences*, vol. 5, no. 3, pp. 157–173, 2015.

[24] Geo-slope International Ltd., "Seep/W User's Guide for Finite Element Seepage Analysis," Calgary, Alberta, Canada, 2007.

[25] D. G. Fredlund and A. Xing, "Equations for the soil-water characteristic curve," *Canadian Geotechnical Journal*, vol. 31, no. 4, pp. 521–532, 1994.

[26] R. J. Kunze, G. Uehara, and K. Graham, "Factors important in the calculation of hydraulic conductivity," *Soil Science Society of America Journal*, vol. 32, no. 6, pp. 760–765, 1968.